



| | |
|------------------|--|
| Title | Local spin moment configuration in the frustrated $s=1/2$ Heisenberg triangular antiferromagnet V15 determined by NMR |
| Author(s) | Furukawa, Yuji; Nishisaka, Yusuke; Kumagai, Ken-ich et al. |
| Citation | Physical Review B, 75(22), 220402 https://doi.org/10.1103/PhysRevB.75.220402 |
| Issue Date | 2007-06-05 |
| Doc URL | https://hdl.handle.net/2115/28418 |
| Rights | Copyright © 2007 American Physical Society |
| Type | journal article |
| File Information | PRB75-22.pdf |



Local spin moment configuration in the frustrated $s=1/2$ Heisenberg triangular antiferromagnet V15 determined by NMR

Yuji Furukawa,¹ Yusuke Nishisaka,¹ Ken-ich Kumagai,¹ Paul Kögerler,^{2,3} and Ferdinando Borsa³

¹*Division of Physics, Graduate School of Science, Hokkaido University, Sapporo 060-0810, Japan*

²*Department of Physics and Astronomy and Ames Laboratory, Iowa State University, Ames, Iowa 50011, USA*

³*Dipartimento di Fisica "A Volta" e Unità CNISM-INFN di Pavia, Via Bassi 6, I27100 Pavia, Italy*

(Received 11 May 2007; published 5 June 2007)

We report very low-temperature measurements of ^{51}V NMR spectra as a function of external magnetic field in the $s=1/2$ Heisenberg triangular antiferromagnet cluster $\text{K}_6[\text{V}_{15}\text{As}_6\text{O}_{42}(\text{H}_2\text{O})]\cdot 8\text{H}_2\text{O}$ (V15), a simple prototype of a geometrically magnetic frustrated system. It is known that the frustration is relieved by a splitting of the degenerate ground state into two $S_T=1/2$ states. Our measurements allow the microscopic determination of the local spin configuration both in the nonfrustrated total spin $S_T=3/2$ state at high fields and in the two quasidegenerate $S_T=1/2$ ground states at low fields, where it is shown that the simple frustrated chiral configuration in the triangle is broken down into two different spin configurations corresponding to the two quasidegenerate $S_T=1/2$ states.

DOI: [10.1103/PhysRevB.75.220402](https://doi.org/10.1103/PhysRevB.75.220402)

PACS number(s): 75.50.Xx, 75.25.+z, 75.75.+a, 76.60.-k

The magnetic properties of antiferromagnets with spin frustration have attracted a great deal of interest because the systems show peculiar properties such as the suppression of the magnetic ordering, unconventional spin states like the spin liquid, and large fluctuations in the ground state. Most of the studies have been performed in three-dimensional magnetic systems such as Kagomé lattice materials and pyrochlores.^{1,2} Usually, most of these materials show short- or long-range magnetic ordering due to small perturbations like defects, anisotropy, and lattice distortions. This prevents the investigation of effects purely associated with spin frustrations. On the other hand, recent progress in synthesizing nanoscale molecular magnets offers the opportunity to investigate the effects of spin frustration at a nanoscale level where "lattice" effects and perturbations are not relevant.³ Molecular magnets are composed of a core of strongly interacting spins localized on transition-metal ions surrounded by large organic ligands, so that each molecular magnet is magnetically isolated from the other molecules. Thus one can investigate the magnetic properties of a system composed of a small number of magnetically coupled spins. $\text{K}_6[\text{V}_{15}\text{As}_6\text{O}_{42}(\text{H}_2\text{O})]\cdot 8\text{H}_2\text{O}$ (V15) is one of the interesting molecular magnets for investigating spin frustration since V15 can be considered a model system for an $s=1/2$ Heisenberg single triangular antiferromagnet.⁴ V15 is comprised of 15 V^{4+} ions with $s=1/2$, which are arranged in a quasi-spherical layered structure with a triangle sandwiched between two hexagons as shown in Fig. 1(a). All exchange interactions between V^{4+} spins are antiferromagnetic (AF).^{5,6} Each hexagon of V15 consists of three pairs of strongly coupled spins with $J_1 \sim 800$ K. Each spin of the V^{4+} ions in the central triangle is coupled with the spins in both hexagons with $J_2=150$ K and $J_3=300$ K,⁸ resulting in a very weak exchange interaction between the spins within the central triangle with $J_0=2.44$ K.⁷ At low temperatures, the magnetic properties of V15 are determined entirely by the three V^{4+} spins on the triangle (a frustrated $s=1/2$ triangular system) because the V^{4+} spins on the hexagon are assumed to form a total $S=0$ spin singlet state due to the strong AF

interaction of $J_1 \sim 800$ K, as confirmed directly by ^{51}V NMR measurements at very low temperatures.⁸

The magnetic levels of V15 at low temperature can thus be described by the simple model spin Hamiltonian

$$H = (J_{12}\mathbf{S}_1 \cdot \mathbf{S}_2 + J_{23}\mathbf{S}_2 \cdot \mathbf{S}_3 + J_{31}\mathbf{S}_3 \cdot \mathbf{S}_1) + g\mu_B\mathbf{H} \cdot (\mathbf{S}_1 + \mathbf{S}_2 + \mathbf{S}_3), \quad (1)$$

where the exchange parameters between spins can be assumed equal in first approximation, i.e., $J_{12}=J_{23}=J_{31}=J_0$, and \mathbf{S}_i are the individual $s=1/2$ V sites. The energy scheme at low temperature is given by a ground state of two degenerate total spins $S_T=1/2$ and an excited state of $S_T=3/2$ which lies ~ 3.8 K above the ground state.⁹ In reality, the two $S_T=1/2$ states are split with a small energy gap, which was estimated to be of the order of 0.08 K from magnetization measurements.¹⁰ Among the possible origins for the gap

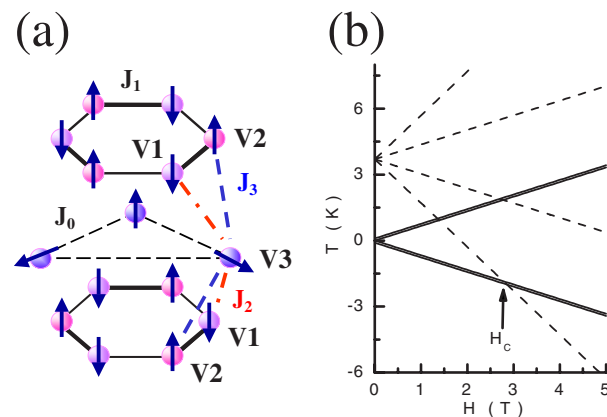


FIG. 1. (Color online) (a) Schematic view of the relative positions of V^{4+} ($s=1/2$) ions (solid circles) and the exchange coupling scheme in V15. (b) Magnetic energy level scheme of V15 as a function of the external magnetic field. Solid and broken lines show the two nearly degenerate $S_T=1/2$ branches and the $S_T=3/2$ branches, respectively.

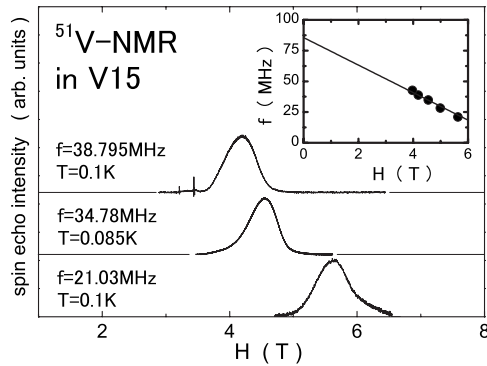


FIG. 2. ^{51}V NMR spectra for the V^{4+} ions in the triangle observed in its $S_T=3/2$ ground states at very low temperature for three different resonance frequencies. The inset shows the external field dependence of the resonance frequency for the peak measured below 100 mK.

are a small Dzyaloshitsky-Moriya (DM) interaction,¹¹ hyperfine interactions,¹² and lattice distortion,¹³ with no consensus yet on the mechanism for the opening of the gap. As shown in Fig. 1(b), by the application of an external magnetic field, the ground state can be changed from the nearly degenerate $S_T=1/2$ frustrated spin states to a nonfrustrated $S_T=3/2$ spin state at a critical field $H_c \sim 2.8$ T. Although the low-lying magnetic spin states are already known there is yet no knowledge about the local spin moment configuration in the ground state, an issue of great relevance in frustrated systems. Nuclear magnetic resonance is known to be a very suitable technique to investigate the static and dynamic magnetic properties in solids in general¹⁴ and in nanoscale molecular magnets in particular.¹⁵

In this Rapid Communication, we report ^{51}V NMR measurements at very low temperature both in the frustrated state at low magnetic fields and in the nonfrustrated state at high magnetic fields. From an analysis of the field dependence of the NMR spectra, we show that the local spin configuration for the different low-lying magnetic states can be determined directly.

A polycrystalline sample of V15 was prepared as described elsewhere¹⁶ and was also used in our previous NMR studies.¹⁷ NMR measurements were carried out using a phase-coherent spin echo pulse spectrometer. The ^{51}V NMR spectra were obtained by sweeping the external magnetic field at constant frequency. The NMR measurements at very low temperature have been carried out using a ^3He - ^4He dilution refrigerator. We address first the problem of the local spin moment configuration in the nonfrustrated excited state. Figure 2 shows ^{51}V NMR spectra at three different resonance frequencies measured at $T \sim 100$ mK in a magnetic field region where the ground state is $S_T=3/2$. With increasing resonance frequency, the peak position of the spectrum shifts to lower magnetic field as shown in the inset of Fig. 2. The resonance frequency f is proportional to the vector sum of the internal field (H_{int}) and external field (H_0):

$$f = \gamma_N(H_0 + H_{\text{int}}) = \gamma_N(H_0 + g\langle s \rangle A), \quad (2)$$

where $\gamma_N/2\pi = 11.285$ MHz/T is the gyromagnetic ratio of the ^{51}V nucleus, and the internal field is expressed as the

product of an isotropic hyperfine contact field A times the local spin density. By fitting the data with Eq. (2), one can derive an internal field $H_{\text{int}} = -76$ kOe. The internal field at the nuclear site in a V^{4+} ion with $s=1/2$ is dominated by the core polarization mechanism, which induces a large negative internal field of the order of 100 kOe/ μ_B at the nuclear site.¹⁸ The value of -76 kOe is close to the value of -85 kOe reported in VO_2 .¹⁹ Thus, this ^{51}V NMR signal can be assigned to V^{4+} ions with $s=1/2$ and $g=2$, i.e., carrying about $1\mu_B$. The smaller hyperfine field in V15 with respect to VO_2 could be due to a slight delocalization of the d wave function in the former compound. In addition, the good fitting result shown by the solid line in the inset of Fig. 2 indicates that the direction of the spin moments for the V ions is parallel to the external field, a result consistent with negligible anisotropy and with the spin densities calculated from the exact diagonalizations of the spin Hamiltonian.²⁰

Quadrupole effects in ^{51}V ($I=5/2$) NMR are present but are irrelevant in our analysis since the quadrupole frequency (ν_Q) must be much smaller than the Zeeman frequency resulting from the sum of the external and internal fields. In fact, ν_Q for the V3 site is estimated to be less than 1 MHz from our calculation of the electric field gradient based on a point charge approximation and using the crystal coordinate data reported previously.²¹ The broadening of the NMR lines is probably due to the anisotropic g value reported to be $g_{\parallel} = 1.981$ and $g_{\perp} = 1.953$.²² This small anisotropy can produce magnetic broadening of the order of 2 kOe, which is of the same order as the experimental observation (~ 6 kOe).

We turn now to the more interesting case of the spin configuration in the frustrated ground state. In the case of a magnetic field less than 2.8 T, where the ground state of V15 is formed by two nearly degenerate $S_T=1/2$ frustrated states, we have succeeded in detecting the ^{51}V NMR signals, which can be observed only below 100 mK due to the very short spin-spin relaxation rate. Typical ^{51}V NMR spectra observed in the $S_T=1/2$ frustrated ground states are shown in Figs. 3(b) and 3(c). The peak position of the spectrum (P1) shown in Fig. 3(b) at different resonance frequencies is plotted as a function of the external field by solid circles in Fig. 3(a). A comparison of the high-field data shown in Fig. 2 with the low-field data [Fig. 3(a)] shows that the two sets of data are almost on the same straight line. Thus we can conclude that the observed low-field ^{51}V NMR signal can be ascribed to V^{4+} ions with almost full spin moments of $1\mu_B$. In addition to the strong signal discussed above, two other low-field ^{51}V NMR signals (P2 and P3) shown in Fig. 3(c) can be observed with relatively weak intensities, whose peak positions at different resonance frequencies are plotted with closed squares (P2) and closed triangles (P3) in Fig. 3(a). In spite of the large experimental uncertainty due to the weak signal intensity and some bending of the data due to uncertainty in the temperature reading in the presence of rf irradiation, one can estimate the internal field for each of the two V^{4+} sites as $-45(2)$ and $+25(2)$ kOe for P2 and P3, respectively, using Eq. (2). Assuming that the hyperfine field for V^{4+} ions in V15 due to the core polarization is -76 kOe for $s=1/2$, one can derive that each of the two additional V^{4+} sites carries a spin moment of about $0.6\mu_B$ and $-0.33\mu_B$ in opposite direc-

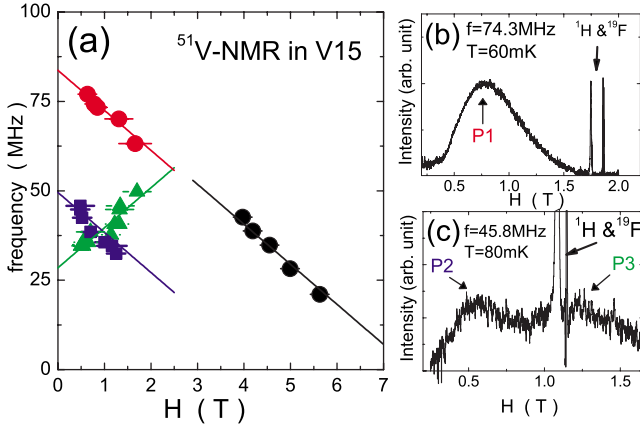


FIG. 3. (Color online) External magnetic field dependence of the resonance frequency for the three ^{51}V NMR signals observed in $S_T=1/2$ ground states at $H_0 < 2$ T. The solid circles represent the stronger signal (P1) shown in (b). The solid squares and triangles refer to the other two weaker signals P2 and P3, respectively, shown in (c). The high-field data in Fig. 2 have been replotted here for comparison (see text). The solid lines show the fitting results as discussed in the text. Typical ^{51}V NMR spectra observed in the $S_T=1/2$ ground states are shown in (b) and (c). The two sharp lines are the ^1H NMR signal from the sample and ^{19}F NMR from Teflon.

tions, where the positive and negative signs of the spin moments correspond to the directions parallel and antiparallel with respect to the external field, respectively. Thus our results indicate the existence in the two quasidegenerate $S_T=1/2$ ground states of three different V^{4+} ions whose spin moments are estimated to be close to $1\mu_B$, $(2/3)\mu_B$, and $-(1/3)\mu_B$.

Let us compare now the experimental findings with the theoretical predictions. The two eigenfunctions for the $s=1/2$ Heisenberg triangular system with spin Hamiltonian Eq. (1) corresponding to the eigenstate given by the two $S_T=1/2$ ground states can be expressed using basis functions of $|S_1 S_2 S_3\rangle$ in which up and down arrows represent up and down spins, respectively, for S_n ,

$$\begin{aligned}\phi_a &= \frac{1}{\sqrt{3}}(|\uparrow\downarrow\downarrow\rangle + \omega|\downarrow\uparrow\downarrow\rangle + \omega^2|\downarrow\downarrow\uparrow\rangle), \\ \phi_b &= \frac{1}{\sqrt{3}}(|\uparrow\downarrow\downarrow\rangle + \omega^2|\downarrow\uparrow\downarrow\rangle + \omega|\downarrow\downarrow\uparrow\rangle),\end{aligned}\quad (3)$$

where $\omega = e^{2\pi i/3}$. These two eigenfunctions correspond to two different spin chiral states in which the V^{4+} spin rotates 120°

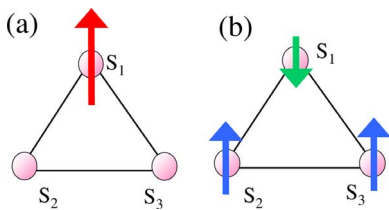


FIG. 4. (Color online) Schematic view of the expectation values for the spin moments for S_1 , S_2 , and S_3 sites on the triangle according to the eigenfunctions (a) ψ_α and (b) ψ_β .

with respect to neighboring spins in clockwise and counter-clockwise directions, respectively, on the triangle. Other eigenfunctions for the same Hamiltonian can be obtained by making linear combinations of the basis functions. The two functions below are also eigenfunctions for the $S_T=1/2$ frustrated spin state:

$$\begin{aligned}\psi_\alpha &= \frac{1}{\sqrt{2}}(|\downarrow\downarrow\uparrow\rangle - |\downarrow\uparrow\downarrow\rangle), \\ \psi_\beta &= \frac{1}{\sqrt{6}}(2|\uparrow\downarrow\downarrow\rangle - |\downarrow\uparrow\downarrow\rangle - |\downarrow\downarrow\uparrow\rangle).\end{aligned}\quad (4)$$

Although the total spin moment for both sets of eigenfunctions [Eqs. (3) and (4)] is $S_T=1/2$ ($1\mu_B$) as required, the expectation values for local spin moments for the S_1 , S_2 , and S_3 sites are estimated to be $1\mu_B$, $0\mu_B$, and $0\mu_B$ for the ψ_α wave function and $-(1/3)\mu_B$, $(2/3)\mu_B$, and $(2/3)\mu_B$ for ψ_β , respectively, as schematically shown in Fig. 4. On the other hand, the expectation values for the local spin moments for the ϕ_a and ϕ_b eigenfunctions in Eq. (3) are calculated to be $(1/3)\mu_B$ for each spin. Since experimentally three V^{4+} ions in the $S_T=1/2$ ground state with different spin moments [$1\mu_B$, $-(1/3)\mu_B$, and $(2/3)\mu_B$] are observed, we conclude that the two eigenfunctions to be associated with the two $S_T=1/2$ ground states can be expressed by ψ_α and ψ_β .²³

Each of the two eigenfunctions should be assigned to one of the two quasidegenerate $S_T=1/2$ ground states. Since the measurements were performed at a temperature smaller than that for the splitting of the two quasidegenerate states, the lower-energy state is more populated and thus yields a larger NMR signal. Since we observe a larger signal intensity for the ^{51}V NMR signal arising from a V^{4+} moment of $1\mu_B$ (see inset in Fig. 3) we conclude that the lower energy of the two $S_T=1/2$ states corresponds to the eigenfunction ψ_α [see Fig. 4(a)]. The other two weak ^{51}V NMR signals [see Fig. 3(c)] arise from V^{4+} ions with moments [$-(1/3)\mu_B$ and $(2/3)\mu_B$] and correspond thus to the eigenfunction ψ_β [see Fig. 4(b)] pertaining to the higher-energy $S_T=1/2$ state. The above conclusions are in agreement with spin density calculations which indicate ψ_α as one of the eigenfunctions for the $S_T=1/2$ ground state.²⁰

Finally we discuss the origin of the splitting of the two $S_T=1/2$ ground states in the V15 cluster. With this aim we have calculated the eigenfunctions and the expectation values of each spin moment for the two $S_T=1/2$ ground states for three possible cases: (1) $J_{12}=J_{31} > J_{23}$, (2) $J_{12}=J_{31} < J_{23}$, and (3) $J_{12}=J_{31}=J_{23}$ with DM interactions. The eigenfunctions for both cases (1) and (2) are given by ψ_α and ψ_β . However, the lower-energy $S_T=1/2$ ground state is ψ_β for case (1) and ψ_α for case (2), respectively. In case (3), DM interaction introduces off-diagonal matrix element which lead to mixings of eigenfunctions between $S_T=1/2$ and $3/2$ states. Although the eigenfunctions for the $S_T=1/2$ states become complicated, we found that the expectation values for spin moments for each $S_T=1/2$ state are the same as the two sets of spin configurations shown in Fig. 4, with the lower-energy state to be associated with the configuration shown in Fig. 4(b). Thus only case (2) is consistent with the

experimental observation that the ground state corresponds to the configuration of Fig. 4(a) or eigenfunction ψ_α . We have made the same calculation for the case of $J_{12} \neq J_{31} \neq J_{23}$. It turns out that only a condition close to case (2) can explain the experimental results. Thus we conclude that the splitting originates from a distortion of the triangle from equilateral to nearly isosceles with exchange constants $J_{12} \sim J_{31} < J_{23}$. Recently, inelastic neutron scattering measurements¹³ conclude that the splitting of the two $S_T = 1/2$ ground states is ascribed to a scalene distortion of the V^{4+} triangle. This conclusion is not inconsistent with the present results, since a scalene distortion with a small difference of J_{12} and J_{31} leads to a spin moment configuration which, within experimental error, cannot be distinguished from the one pertaining to an isosceles distortion.

In summary, we have carried out ^{51}V NMR measurements in $\text{K}_6[\text{V}_{15}\text{As}_6\text{O}_{42}(\text{H}_2\text{O})] \cdot 8\text{H}_2\text{O}$, a model system of a $s=1/2$ Heisenberg triangular antiferromagnet. The measurements at very low temperature and as a function of the external applied field have allowed the determination of the local microscopic spin configuration in the frustrated ground state. It is found that the pure chiral states described by Eq. (3) is broken down in the V15 cluster. The two quasidegenerate

$S_T=1/2$ ground states correspond to two different spin configurations which can be described by the two eigenfunctions ψ_α and ψ_β . We also found that the lower energy of the two $S_T=1/2$ split states is the one pertaining to the eigenfunction ψ_α . The local spin configuration is consistent with a small structural distortion from an equilateral triangle to a nearly isosceles one. It is pointed out that NMR appears to be a unique tool for this kind of model-independent determination of the local spin configuration in frustrated systems.

The present work was in part supported by the 21st Century COE Program ‘‘Topological Science and Technology’’ at Hokkaido University and Grant-in-Aid for Scientific Research on Priority Areas ‘‘High Field Spin Science in 100 T’’ (No. 451) and for Scientific Research (C) from the Ministry of Education, Culture, Sports, Science and Technology of Japan. One of the authors (Y.F.) also thanks K. Nemoto for fruitful discussions and the Sumitomo Foundation for financial supports. Ames Laboratory is operated for U.S. Department of Energy by Iowa State University under Contract No. W-7405-Eng-82. This work at Ames Laboratory was supported by the Director for Energy Research. The work in Pavia was supported by NOE-MAGMAGNET.

¹For a review, see G. Misguich and C. Lhuillier, in *Frustrated Spin Systems*, edited by H. T. Diep (World Scientific, Singapore, (2005)).

²R. Moessner and J. T. Chalker, *Phys. Rev. Lett.* **80**, 2929 (1998).

³D. Gatteschi, R. Sessoli, and J. Villain, *Molecular Nanomagnets* (Oxford University Press, Oxford, (2006)).

⁴D. Gatteschi, L. Pardi, A. L. Barra, A. Müller, and J. Döring, *Nature* (London) **354**, 463 (1991).

⁵D. Gatteschi, L. Pardi, A. L. Barra, and A. Müller, *Mol. Eng.* **3**, 157 (1993).

⁶A. L. Barra, D. Gatteschi, L. Pardi, A. Müller, and J. Döring, *J. Am. Chem. Soc.* **114**, 8509 (1992).

⁷G. Chaboussant, R. Basler, A. Sieber, S. T. Ochsenbein, A. Desmedt, R. E. Lechner, M. T. F. Telling, P. Kögerler, A. Müller, and H.-U. Güdel, *Europhys. Lett.* **59**, 291 (2002).

⁸Y. Nishisaka, Y. Furukawa, K. Kumagai, and P. P. Kögerler, in *Low Temperature Physics*, edited by Y. Takano, S. P. Hershfield, S. O. Hill, P. J. Hirschfeld, and A. M. Goldman, *AIP Conf. Proc.* No. 850 (AIP, Melville, 2006), p. 1145.

⁹V. V. Dobrovitski, M. I. Katsnelson, and B. N. Harmon, *Phys. Rev. Lett.* **84**, 3458 (2000).

¹⁰I. Chiorescu, W. Wernsdorfer, A. Müller, H. Bögge, and B. Barbara, *Phys. Rev. Lett.* **84**, 3454 (2000).

¹¹I. Chiorescu, W. Wernsdorfer, B. Barbara, A. Müller, and H. Bögge, *J. Magn. Magn. Mater.* **221**, 103 (2000); S. Miyashita and N. Nagaosa, *Prog. Theor. Phys.* **106**, 533 (2001); H. De Raedt, S. Miyashita, K. Michielsen, and M. Machida, *Phys. Rev. B* **70**, 064401 (2004).

¹²S. Miyashita, H. De Raedt, and K. Michielsen, *Prog. Theor. Phys.* **110**, 889 (2003).

¹³G. Chaboussant, S. T. Ochsenbein, A. Sieber, H.-U. Güdel, H. Mutka, A. Müller, and B. Barbara, *Europhys. Lett.* **66**, 423 (2004).

¹⁴F. Borsa and A. Rigamonti, *Local Properties of Phase Transitions*, edited by K. A. Müller and A. Rigamonti (Pergamon Press, Oxford, 1976).

¹⁵F. Borsa, A. Lascialfari, and Y. Furukawa, in *Novel NMR and EPR Techniques*, edited by J. Doliněk, M. Vifan, and S. Žumer (Springer, Berlin, 2006).

¹⁶J. Choi, L. A. W. Sanderson, J. L. Musfeldt, A. Ellern, and P. Kögerler, *Phys. Rev. B* **68**, 064412 (2003).

¹⁷Y. Furukawa, Y. Fujiyoshi, K. Kumagai, and P. Kögerler, *Polyhedron* **24**, 2737 (2005); D. Procissi, A. Lascialfari, E. Micotti, M. Bertassi, P. Carretta, Y. Furukawa, and P. Kögerler, *Phys. Rev. B* **73**, 184417 (2006).

¹⁸R. E. Watson and A. J. Freeman, in *Hyperfine Interactions*, edited by A. J. Freeman and R. B. Frankel (Academic Press, New York, (1967)).

¹⁹K. Takanaishi, H. Yasuoka, Y. Ueda, and K. Kosuge, *J. Phys. Soc. Jpn.* **52**, 3953 (1983).

²⁰C. Raghun, I. Rudra, D. Sen, and S. Ramasesha, *Phys. Rev. B* **64**, 064419 (2001).

²¹A. Müller and J. Döring, *Z. Anorg. Allg. Chem.* **595**, 251 (1991).

²²S. Vongtragool, B. Gorshunov, A. A. Mukhin, J. van Slageren, M. Dressel, and A. Müller, *Phys. Chem. Chem. Phys.* **5**, 2778 (2003).

²³Strictly speaking, a linear combination of Eq. (4) would still represent eigenfunctions for the $S_T=1/2$ ground state. The degree of mixing of ψ_α and ψ_β , depends on the values of the exchange coupling constants.